CMLS, Cell. Mol. Life Sci. 59 (2002) 2136–2143
1420-682X/02/122136-08

CMLS Cellular and Molecular Life Sciences

Research Article

Active-site mutants of class B β-lactamases: substrate binding and mechanistic study

C. Prosperi-Meys[a,b,*], D. de Seny[b], G. Llabres[a], M. Galleni[b] and J. Lamotte-Brasseur[b,c]

[a] Service de Physique Expérimentale, Institut de Physique (B5), University of Liège, Sart-Tilman, 4000 Liège (Belgium), Fax +32 4 3662813, e-mail: christelle.prosperi@ulg.ac.be
[b] Centre d'Ingénierie des Protéines, Institut de Chimie (B6), University of Liège, Sart-Tilman, 4000 Liège (Belgium)
[c] Unité de Cristallographie, Institut de Physique (B5), University of Liège, Sart-Tilman, 4000 Liège (Belgium)

Received 28 August 2002; received after revision 22 October 2002; accepted 24 October 2002

Abstract. Increased resistance to β-lactam antibiotics is mainly due to β-lactamases. X-ray structures of zinc β-lactamases unraveled the coordination of the metal ions, but their mode of action remains unclear. Recently, enzymes in which one of the zinc ligands was mutated have been characterized and their catalytic activity against several β-lactam antibiotics measured. A molecular modeling study of these enzymes was performed here to explain the catalytic activity of the mutants. Coordination around the zinc ions influences the way the tetrahedral intermediate is bound; any modification influences the first recognition of the substrate by the enzyme. For all the studied mutants, at least one of the interactions fails, inducing a loss of catalytic efficiency compared to the wild type. The present studies show that the enzyme cavity is a structure of high plasticity both structurally and mechanistically and that local modifications may propagate its effects far from the mutated amino acid.

Key words. Catalytic mechanism; metallo-β-lactamase; molecular mechanics; molecular modeling; penicillin binding; zinc enzyme.

The most common cause of antibiotic resistance is the production of bacterial enzymes which hydrolyse β-lactams to an inactive form [1]. Four classes of β-lactamases have been defined depending on amino acid sequence similarities. Class A, C, and D β-lactamases are serine enzymes, while class B contains metallo-β-lactamases. Zinc-β-lactamases do not share any sequence or structure similarity with active-site serine β-lactamases.

The increase in resistance to β-lactam antibiotics and the broad activity spectrum of metallo-β-lactamases in many pathogenic bacteria are especially frightening. They are unselective and hydrolyze almost all β-lactam drugs designed so far excepted monobactams. They comprise three different structural classes exhibiting considerable sequence diversity despite the conservation of some motifs. The most populated is class B1, containing enzymes that share relatively high sequence similarity to the *Bacillus cereus* and *Bacteroides fragilis* enzymes and the plasmid-borne IMP-1 enzyme, whose three-dimensional structures have been elucidated [2–7].

No crystal structure is known for the *Aeromonas* enzymes of class B2, but the structure of the class B3 *Stenotrophomonas maltophilia* β-lactamase showed a similar protein fold [8]. Class B β-lactamases contain two metal-binding sites [9] and in the *B. cereus* enzyme, the two zinc ions are liganted by active-site residues that are generally conserved in all known B1 metallo-β-lactamase sequences.

The number of zinc ions required for optimal activity varies within the Zn-β-lactamase family; how these dif-

* Corresponding author.

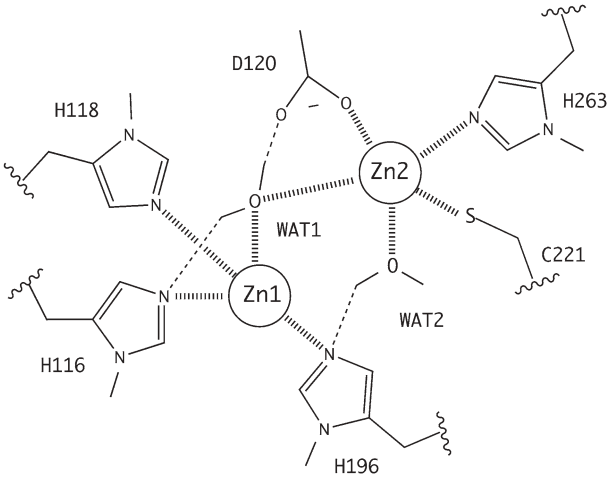

Figure 1. Schematic representation of the zinc-binding sites of the *B. cereus* β-lactamase. The hatched lines show the coordination sphere of the zinc ions and the dotted lines show electrostatic interactions between atoms.

ferent requirements translate into the mechanism of these enzymes remains an open question.

In the first binding site (the 'three-His' site), the zinc ion is tetrahedrally coordinated by three equivalent histidine residues (His^{116}, His^{118}, and His^{196}) and a single water molecule (WAT1) (fig. 1). In the so-called 'Cys site,' the second zinc ion is coordinated in a pentavalent distorted trigonal bipyramidal conformation by the same water molecule (which thus 'bridges' the two zinc ions), one further water molecule (WAT2), and an Asp^{120}-Cys^{221}-His^{263} triad, which is conserved across the class B1 metallo-β-lactamase sequences. Even in enzymes containing one equivalent of zinc per molecule, zinc is distributed between both available binding sites [10]. The zinc ions would then move from the three-histidines site to the cysteine site, the population of either site depending on the zinc concentration and the pH. The di-zinc form of the *B.cereus* enzyme is used in this study.

Recently, enzymes in which one of the zinc ligands has been mutated have been characterized and their catalytic activity against several β-lactam antibiotics measured (table 1) [11]. In a recent paper, geometry optimization of stable complexes along the reaction pathway of benzylpenicillin highlighted a proton shuttle implicating Asp^{120}, the two water molecules, and Zn2. The catalytic role of Zn2 and the flexibility in the coordination geometry of both Zn ions was of crucial importance for catalysis [12]. To analyze the relative catalytic importance of both binding sites, a molecular modeling study of a set of amino acid substitutions of the zinc ligands was performed here. The effect of these mutations in the active site and the consequences for the catalytic mechanism were analyzed. This work also confirmed the proposed importance of several amino acid residues in the catalytic mechanism of class B β-lactamases.

Materials and methods

Modeling of protein structures

All calculations were based on the high-resolution X-ray structure of *B. cereus* from crystals obtained at pH 7.5, as described in Prosperi-Meys et al. [12]. Histidines present in the active site were taken as neutral. For the other three histidines, the tautomeric form of the imidazole ring was chosen according to the X-ray structure, after geometrical analysis of the potential hydrogen bonds. The Zn2-coordinated cysteine was in the thiolate form. Other titratable sites were assigned their usual protonation states at pH 7. Hydrogen atoms were added to the crystal structure using the PROTONATE module of AMBER 4.1 [13]. The BBL numbering [14] has been used throughout this paper. The molecular structures were manipulated with InsightII (Molecular Simulations, San Diego, Calif.).

Table 1. Kinetic parameters against benzylpenicillin and zinc ion content for the wild-type enzyme and zinc ion content for the wild-type (WT) and mutant enzymes [11].

	Benzylpenicillin[a]			
	K_m (%WT)	k_{cat} (%WT)	k_{cat}/K_m (%WT)	[Zn]/[E][b]
WT	100	100	100	1,7
H116S	305	20	6,5	2
H118S	1340	15	0,9	1,7
D120N	260	1,5	0,6	1,6
H196S	3310	3	0,09	1,7
C221S	280	6	2,3	–
C221S[b]	450	87	19	1,7
H263S	>3490	>6	–	1,1

[a] [ZnSO4] in the buffer = 0.4 µM.
[b] [ZnSO4] in the buffer = 100 µM.

His → Ser mutants

Models of the mutant enzymes were obtained from the X-ray structure of the wild-type protein. For all His → Ser mutants, three Cα-Cβ torsion angles were considered, the first one leading to the shortest possible Oγ-Zn distance, the other two differing from the first by rotations of 120 and 240°, respectively. The geometry of each structure was then optimized by energy minimization as described below.

C221S mutant

The X-ray structure of the *B. cereus* and *B. fragilis* C221S mutant β-lactamases are known [15], but the coordinates were not suitable for modeling: both structures only contained one zinc ion (due to the crystallization conditions) and a sodium citrate ion was present in the *B. cereus* active site. In the model structures, three starting conformations of the serine side chain were taken into account as for the His→Ser mutations (see above).

D120N mutant

The local conformational space of the mutated Asn[120] was searched by a minimal-perturbation approach method [16]. A conformational map was calculated by 30° steps around the Cα-Cβ and Cβ-Cγ bonds (data not shown). The two minima found in the map were chosen as starting conformations for the minimization procedure described hereafter.

Benzylpenicillin model

The geometry of benzylpenicillin and of the benzylpenicillin tetrahedral intermediate was optimized by the AM1 semi-empirical method [17] and docked into the mutant enzyme active site as described in Prosperi-Meys et al. [12]. The starting position of the benzylpenicillin tetrahedral intermediate was that of the benzylpenicillin in the optimized complexes.

The energy of the corresponding complexes was minimized as described for the native enzyme with the use of CNDO charges to compute the coulombic term. The bond lengths, and bond and dihedral angles of these entities were constrained to the AM1 values while allowing rotation around the free bonds.

Molecular-mechanics calculations

The molecular-mechanics potential parameters and minimization strategy were as described in Prosperi-Meys et al. [12] for the wild-type enzyme.

Results

All calculations were based on the high-resolution X-ray structure of *B. cereus* from crystals obtained at pH 7.5, as described in Prosperi-Meys et al. [12].

For all His→Ser and the Cys→Ser mutants, three Cα-Cβ torsion angles were considered. Two different starting conformations were chosen for the Asn[120] side chain. The geometry of each structure was then optimized by energy minimization (for details, see Materials and methods).

A single orientation of the serine side chain was found after minimization of the serine mutant structures. In the His→Ser mutant models, the serine dihedral angles around the Cα-Cβ bond were 76°, –167°, 69°, and –176° for Ser[116], Ser[118], Ser[196], and Ser[263], respectively, in agreement with those (around –180°, –60°, and 60°) commonly adopted by serine residues [18].

With the exception of the environment of the mutation site, there were no major differences between the structure of wild-type and mutant enzymes (root mean square distances between pairs of Cα atoms between 0.08 and 0.15 Å).

Conservation of the coordination around both zinc ions depended on the mutated residue. In turn, the position of the water molecules and/or of the other zinc ligands sometimes changed, occasionally modifying profoundly the relative disposition of catalytically important functional groups. Superimposition of the different structures showed that some Zn ligands moved more than others.

The His[116] and Cys[221] residues appeared as highly mobile. This flexibility might be due to the fact that they interact loosely via hydrogen bonds with the rest of the protein. These residues remained, however, in strong interaction with the zinc ions (table 2). When they were mutated into serine, they kept coordination with the zinc, and the geometry of the active site was barely disrupted.

By contrast, the His[196] and His[263] side chains remained fixed at an almost unique position in the mutants. On the other side of the imidazole rings, the protonated nitrogens of these histidines were involved in strong hydrogen-bonding interactions (His[196] with the backbone oxygen atoms of Asn[180], via a conserved water molecule, and His[263] with the backbone oxygen of the generally conserved Pro[40]). This might explain the relative rigidity of these zinc ligands. In these mutant structures, the serine side chains lose all interaction with the zinc, thus disrupting the coordination around the metal ion.

His[118] is an intermediate case; it was hydrogen-bonded to the Asp[183] side chain, which can move easily around the Cβ-Cγ bond. His[118] was thus allowed to move somewhat more than the two histidines described above. Ser[118] remained a ligand of Zn1.

The enzyme-substrate models

In the Henri-Michaelis complex models, a benzylpenicillin molecule was docked in the mutant enzyme active site (for details, see Materials and methods). Unless otherwise stated, binding of the substrate did not modify the features described above for the free enzymes.

Table 2. Some relevant atom-atom distances (in A) measured in each model.

	WT	H116S	H118S	H196S	H263S	D120N	C221S
Zn1-Zn2	3.35	3.81	3.16	3.2	3.44	3.41	3.22
Zn1-N(H116)	2.21	1.93[a]	2.21	2.2	2.2	2.27	2.21
Zn1-N(H118)	2.09	2.21	3.18[a]	2.21	2.2	2.07	2.05
Zn1-N(H196)	2.05	2.2	2.2	5.06[a]	2.2	2.08	2.04
Zn2-N(H263)	2.21	2.21	2.2	2.2	6.67[b]	2.21	2.21
Zn2-S(C221)	2.78	2.37	2.37	2.37	2.37	3.46	1.92[b]
Zn2-OD1(D120)	2.92	2.24	2.24	2.24	2.25	2.48	2.87
Zn1-WAT1	1.95	2.04	1.91	1.97	1.95	2.03	1.93
Zn2-WAT1	2.11	2.12	2.11	2.02	2	1.97	1.98
Zn2-WAT2	2	1.98	1.96	2	1.94	1.92	3.64
WAT1-WAT2	2.82	2.94	2.91	2.93	3.67	3.14	2.52

[a] Zn1-Oγ(SER).
[b] Zn2-Oγ(SER).

As described in Prosperi-Meys et al. [12], the lactam carbonyl oxygen atom was located in an oxyanion hole formed by the side chain Nδ group of Asn[233] and the Zn1 ion (fig. 2). The antibiotic carboxylic group interacted losely with the Lys[224] ammonium group, the carbonyl oxygen of the penicillin acetamido side chain was hydrogen-bonded to the backbone NH groups of residues Ala[119] and Asp[120]. The phenyl group of penicillin was located in a hydrophobic pocket formed by the side chains of Phe[61] and Trp[87]. The thiazolidine methyl groups interacted with Val[67].

None of these residues was disturbed by the mutations, and the main substrate-binding features were also valid for the considered mutants. These results confirmed that the mutated residues were not directly involved in the orientation of the β-lactam molecule in the enzyme cavity.

When the Zn1-carbonyl interaction polarizes the C–O bond, WAT1 can readily attack the carbonyl carbon of the substrate (fig. 3 A, step 1) while the Asp[120] carboxylate might accept a proton from this water molecule, thus also promoting the attack (fig. 3 A, step 2). The lactam carbonyl carbon adopts a tetrahedral geometry. In this tran-

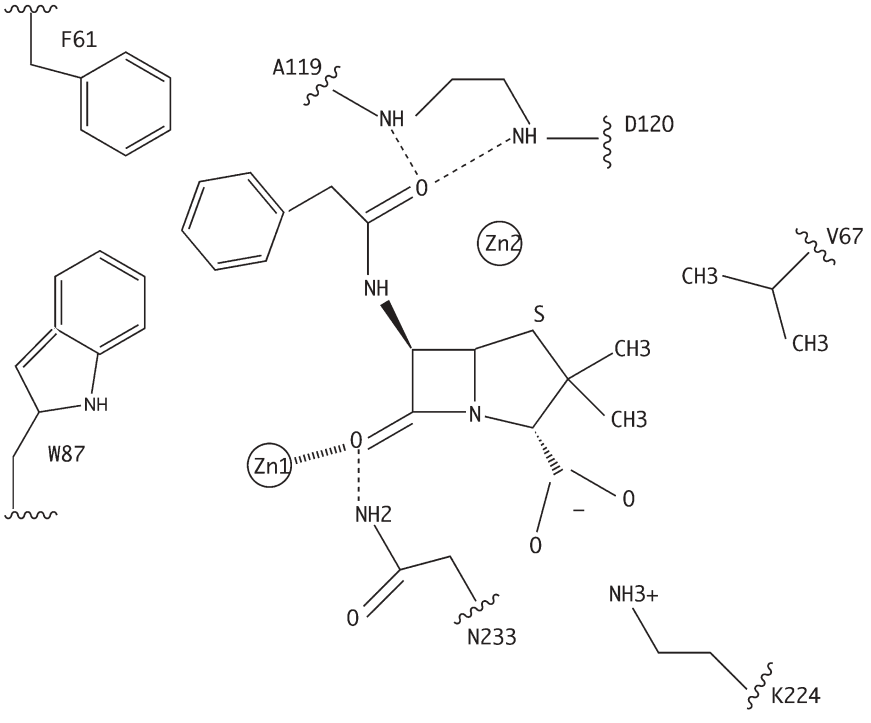

Figure 2. Starting geometry for the docking of benzylpenicillin in the enzyme active site, as used for energy minimization of the complexes.

Table 3. Distances measured (in Å) in the tetrahedral intermediate with benzylpenicillin.

	WT	H116S	H118S	H196S	C221S
Zn1-Olact	2,64	2,63	2,96	3,27	2,62
O(WAT1)-Clact	3,35	3,16	3,25	3,26	3,04
O(WAT1)-Od1(D120)	2,42	2,39	2,41	2,38	2,38
Zn2-Od2(D120)	2,04	2,18	2	1,95	1,94
Zn2-Nlact	2,2	2,31	2,76	3,33	4,07

sient (but crucial) step, the breaking and forming of bonds were accompanied by a charge reorganization inducing a rapid proton transfer to the lactam nitrogen.
In the wild-type enzyme, this step was characterized by a displacement of Zn2 toward the lactam nitrogen atom (fig. 3 B, step 3). The Zn2-Nlact distance shortened down to 2.2 Å, so that the nitrogen became a new ligand of Zn2. For efficient catalysis, the path of the proton should be optimal and the distances between the atoms involved in the shuttle short enough for the transfer to occur easily. Figure 3 A, B shows the atoms supposed to be involved in the proton shuttle and the distances between them as found in the case of the wild-type enzyme (table 3). Such an ideal proton transfer depends mainly on the position of the zinc ions, which act as central attraction points for the ligands.
We will now describe the structural modifications characteristic of each mutant model and discuss the way they could influence the catalytic mechanism. The distances are given in tables 2 and 3 while the modifications of the catalytic constants are from table 1.

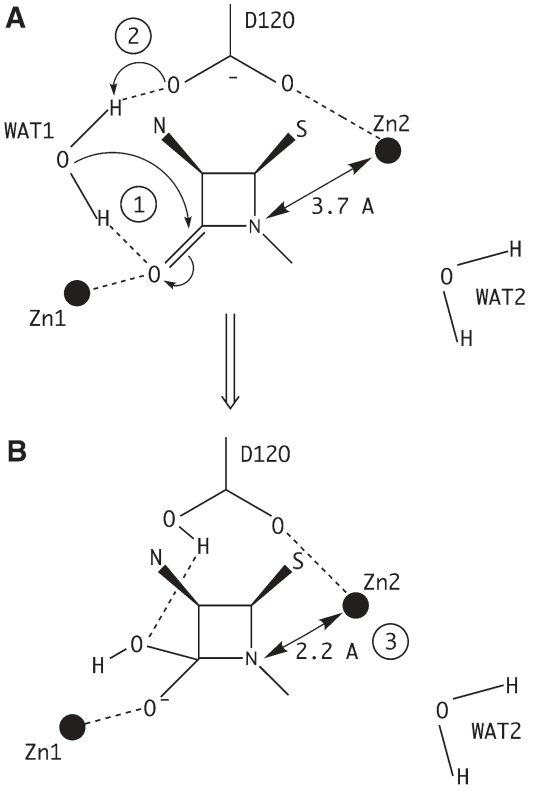

Figure 3. Schematic representation of the atoms supposed to be involved in the proton shuttle in different steps of the reaction: Henri-Michaelis complex with benzylpenicillin (*A*); tetrahedral intermediate (*B*). The arrows show the proposed electron shifts and the dotted lines show electrostatic interactions between atoms. The encircled numbers 1, 2, and 3 represent the catalytic steps of the reaction, as discussed in the text.

Mutants of the 'three His site'

1) H116S enzyme

The Ser^{116} side chain oxygen interacted with Zn1. The zinc coordination remained tetrahedral, His^{196} moved with Zn1 and the His^{196}-WAT2 hydrogen bond disappeared. As a result, WAT2 bound in a somewhat altered position, keeping, however, the square bipyramidal coordination of the Zn2.
Due to the conservation of the coordination around both zinc ions, the binding of benzylpenicillin was found to be similar to that in the wild-type enzyme (table 3) and the K_m value was low. The Zn2-Asp^{120} Oδ and Zn2-Nlact distances increased slightly with respect to those obtained in the case of the wild-type enzyme. The proton shuttle should occur somewhat less easily, and indeed the k_{cat} value was five times lower than that of the wild type.

2) H118S enzyme

The Ser^{118} hydroxyl group turned toward His^{116} and WAT1. Interacting with the Ser^{118} Oγ atom, WAT1 moved outside the plane of the Asp^{120} carboxylate group, which in turn rotated away from the active site. Reorganization of the hydrogen-bonding network became distorted but maintained the coordination around both Zn1 and Zn2. The His^{196}-WAT2 bond disappeared (K_m value increases). The carbonyl oxygen of the lactam bound 0.3 Å further from Zn1, and a 0.6-Å increase in the Zn2-Nlact distance can be correlated with the sixfold decrease in the k_{cat} value.

3) H196S enzyme

The structure of this mutant was the most affected by the mutation. The first zinc ion lost the Ser^{196} ligand, whose hydroxyl group was turned toward Asp^{230} Oδ. The Zn1 coordination was thus profoundly modified. WAT2 be-

came hydrogen-bonded to His^{263} (instead of His^{196}), and the Zn2 coordination was also slightly altered.
The empty space left by the histidine side chain allows the benzylpenicillin molecule to translate 0.8 Å from its initial position in the wild-type complex. The Phe^{61}-phenyl and the Val^{67}-thiazolidine methyl interactions thus disappear and the K_m value increases accordingly.
Even more deleterious to catalysis is the 1-Å increase in the Zn2-Nlact distance, and the k_{cat} value decreases 30-fold.

Mutants of the 'Cys' binding site

1) H263S enzyme

In this model, the Ser^{263} side chain was oriented away from Zn2 and from the active site (table 2). The mutation has then left a very large cavity in the mutant active site. WAT2 occupied the site of the His^{263} imidazole in the wild-type enzyme. WAT1 remained in the tetrahedral coordination sphere of Zn1. However, the Zn2 coordination was affected, as His^{263} was no longer a ligand. This might explain why the H263S mutant was unable to bind more than 1.1 equivalents of zinc, even in the presence of 100 µM Zn^{2+} in the buffer [11]. There is not enough zinc to play a role in the proton shuttle, and the k_{cat} value against benzylpenicillin is drastically decreased (table 1). The perturbation of the active site geometry is directly responsible for the high K_m value.

2) C221S enzyme

With no zinc added to the buffer, the k_{cat} value of this mutant against benzylpenicillin remained very low, probably due to the absence of zinc in the second binding site, which is involved in the catalytic mechanism. Unlike the results obtained for the H263S mutant, the zinc ion content of the C221S mutant can be increased by addition of Zn^{2+} to the buffer, and was accompanied by a higher k_{cat}, showing a correlation between these two features. In the C221S mutant model, the Ser^{221} residue side chain occupied the same site as that of Cys^{221} in the wild-type enzyme.
The torsion angle about Cα-Cβ (–48°) was similar to that of the cysteine in the wild-type enzyme (–51°) and to those found in the C221S β-lactamase structures (–48°) [15, 19].
All side chains that were coordinated to either metal ion in the wild-type enzyme occupied the same position in the mutant, and the benzylpenicillin molecule bound as in the wild-type complex.
Surprisingly, modeling of the tetrahedral intermediate did not give rise to a complex in which the Zn ion was located close to the lactam nitrogen, as found for the mutants of the first binding site. For this model, the coordination around the Zn2 ion became tetrahedral, with the WAT2 water molecule forming the fourth vertex, being located between Zn2 and the lactam nitrogen (Zn2-OWAT2 1.9 Å, OWAT2-Nlact 2.7 Å). Thus WAT2 seemed to be the final relay in the proton shuttle (between Asp^{120} and the lactam nitrogen via Zn2), allowing an efficient hydrolysis of benzylpenicillin when the zinc content is sufficiently high.

3) D120N enzyme

Asparagine is considered to be a conservative substitution for aspartic acid in terms of size. It is therefore an improbable effector of catastrophic structural changes.
Two minima were found in the conformational map. In the two conformers, the Cβ-Cγ torsion angle of Asn^{120} differed by 180° (see Materials and methods). In both minimized structures, the Asn^{120} Oδ atom remained a ligand of Zn2, thus explaining why the zinc-binding capability of the mutant was unaltered [11].
The NδH2 groups were oriented further from Zn2. Due to the reorganization of the active-site geometry, both zinc atoms and both water molecules were bound in slightly altered positions. In the most stable conformer (Asp^{120} N1), the NδH2 group was oriented toward the antibiotic-binding site and H-bonded to WAT1. Instead of a salt bridge, the guanidinium group of Arg^{121} formed a double H bond with Asp^{120}Oδ. In the less stable structure (Asp^{120}N2), the NH2 group was oriented to and H-bonded with one of the Arg^{121}Nη, and the Arg side chain was reoriented. WAT1 still interacted with Asn^{120} Oδ but not with Zn2.
The position of benzylpenicillin in the Asp^{120}N1 model was quite similar to that found in the model of the complex with the wild-type enzyme. By contrast, in the Asp^{120}N2 model, the benzylpenicillin lactam ring rotated (about 20°) around the lactam carbonyl oxygen kept in the oxyanion hole. As a consequence of this rotation, the acetamido side chain of the substrate did not correctly interact with the backbone amide hydrogen atoms of residues 119 and 120. The almost unaffected alteration of the K_m values (table 1) of this mutant with respect to benzylpenicillin are in good agreement with the features of the Asp^{120}N1 model. We thus considered the Asp^{120}N1 model as the most probable one, in agreement with the lower energy of this structure.
Finally, the nucleophilic attack by WAT1 should be accompanied by the transfer of one of its protons to the carboxylate of Asp^{120}.
Conversion of the negatively charged aspartic acid residue by a neutral asparagine would prevent this transfer. This should severely impair the catalytic process, as observed experimentally.

Discussion

The synthesis of potent broad-spectrum and selective inhibitors of β-lactamases has always been a contest be-

tween chemists and bacteria. To date, all the effective and clinically used inhibitors of serine β-lactamases are rapidly hydrolyzed by metallo-β-lactamases. The present investigation contributes new insights with respect to this discussion. In this paper our goal was to analyze the impact of the mutations on the enzyme structure and coordination of zinc, and to show how these modifications could influence the catalytic efficiency of the *B. cereus* enzyme.

First, enzymes from different bacterial strains clearly exhibit distinctive metal-binding affinities, and each zinc site may play a specific role in the enzyme activity. However, with the exception of metallo-β-lactamases isolated from *Aeromonas* species, the presence of two equivalents of metal ion does not strongly modify the catalytic efficiency of the enzymes. The high similarity of the binuclear active sites of *B. fragilis* and *B. cereus* does not correlate with the distinct binding affinities of these enzymes toward bivalent cations. The analysis of Yang et al. [20] showed clearly that the zinc content was not the only factor contributing to the observed changes in the enzymatic activity of the mutants of the *B. fragilis* enzyme.

Moreover, all kinetic measurements indicate that many of the substituted amino acids play a critical role in the enzymatic function of the protein. The most dramatic effects were observed when the enzyme harbored an amino acid substitution of one of the zinc ligands. Kinetic parameters for the D120N mutants are of the same order in the *B. cereus* and *B. fragilis* enzymes. This confirms the critical role played by the Asp^{120} residue in the proton shuttle. Conversion of the negatively charged aspartic acid residue into a neutral asparagine severely impairs the catalytic process regardless of what directly surrounds the aspartic residue (R121 in *B. cereus* and C121 in *B. fragilis*).

As mentioned in Prosperi-Meys et al. [12], in the metallo-β-lactamases, as in other metallo-enzymes, the Zn ions have essentially two roles: a structural role in stabilizing the local conformation and/or an active role in catalysis.

For all the studied mutants, the Zn1 ion retained a structural role in maintaining WAT1 and WAT2, either directly or through the Zn1 tetrahedrally coordinated histidine ligands. The Zn2 ion has a more catalytic role, by stabilizing the tetrahedral intermediate and accepting the β-lactam nitrogen atom as a ligand.

In this paper, we showed how the modification of the structure and the coordination of the zinc could influence the catalytic efficiency of the *B. cereus* enzyme.

The coordination around Zn2 ions influences the way the tetrahedral intermediate is bound, due to the interaction between Zn2 and the lactam nitrogen. Any modification in the zinc coordination thus influences the recognition of the substrate by the enzyme. For all of the studied mutants, at least one of the interactions mentioned above fails, inducing a loss of catalytic efficiency toward all the studied substrates, compared to the wild type.

Indeed, the catalytic pathway described here for penicillins should also be valid for cephalosporins, though in this case, hydrolysis is followed by elimination of the C3 leaving group [21]. This side chain would extend between loops L1 (residues 61–68) and L3 (residues 227–231) [14]. The enzyme-substrate interactions thus strongly depend on the cephalosporin side chain and on the amino acids in the loops, which are specific to each enzyme. This remark also applies to the side chains at C6 of the carbapenem compounds, which are generally considered as poor substrates of the zinc β-lactamases [22]. So far, few compounds have been proposed as potential inhibitors of these enzymes [23–25] but we intend to check and refine our model taking these molecules into consideration, as soon as the kinetic parameters are determined.

In conclusion, the present studies show that, owing to the high density of the hydrogen-bonding network, the enzyme cavity is a structure of high plasticity both structurally and mechanistically. Local modifications that cause the disappearance or weakening of any zinc ligand may propagate their effects far from the mutated amino acid. Due to the closed shell of d10 electrons around the zinc ions, stabilization of the different active-site ligands may occur by changes in the Zn-ligand bond, distances, and angles.

We could also say that the basic structural features required for β-lactamase activity are already well defined in *B. cereus*. Other enzymes, such as those of *B. fragilis* or *S. maltophilia* may possess more exquisite features shaped by different evolutionary pressures that still need to be explored.

Specific nuclear magnetic resonance experiments using all the mutants mentioned in this paper are in progress to confirm the results of this study.

Acknowledgements. This work was supported in part by the European Training and Mobility of Researchers Program (CT98-0232) and by the Belgian Program Pôles d'Attraction Interuniversitaire initiated by the Belgian State, Prime Minister's Office, Services Fédéraux des Affaires Economiques, Techniques et Culturelles (PAI P4/03). The authors thank Professor J.-M. Frère for many insightful discussions.

1 Wang Z., Fast W., Valentine A. M. and Benkovic S. J. (1999) Metallo-β-lactamase: structure and mechanism. Curr. Opin. Chem. Biol. **3:** 614–622

2 Carfi A., Pares S., Duee E., Galleni M., Duez C., Frere J. M. et al. (1995) The 3-D structure of a zinc metallo-β-lactamase from *Bacillus cereus* reveals a new type of protein fold. EMBO J. **14:** 4914–4921

3 Carfi A., Duee E., Paul-Soto R., Galleni M., Frere J. M. and Dideberg O. (1998) X-ray structure of the ZnII beta-lactamase from *Bacteroides fragilis* in an orthorhombic crystal form. Acta Crystallogr. D Biol. Crystallogr. **54:** 45–57

4 Carfi A., Duee E., Galleni M., Frere J.-M. and Dideberg O. (1998) 1.85 Å resolution structure of the zincII β-lactamase from *Bacillus cereus*. Acta Crystallogr. D Biol. Crystallogr. **D54:** 313–323

5 Fabiane S. M., Sohi M. K., Wan T., Payne D. J., Bateson J. H., Mitchell T. et al. (1998) Crystal structure of the zinc-dependent beta-lactamase from *Bacillus cereus* at 1.9 Å resolution: binuclear active site with features of a mononuclear enzyme. Biochemistry **37:** 12404–12411

6 Concha N. O., Rasmussen B. A., Bush K. and Herzberg O. (1996) Crystal structure of the wide-spectrum binuclear zinc beta-lactamase from *Bacteroides fragilis*. Structure **4:** 823–836

7 Concha N. O., Janson C. A., Rowling P., Pearson S., Cheever C. A., Clarke B. P. et al. (2000) Crystal structure of the IMP-1 metallo beta-lactamase from *Pseudomonas aeruginosa* and its complex with a mercaptocarboxylate inhibitor: binding determinants of a potent, broad-spectrum inhibitor. Biochemistry **39:** 4288–4298

8 Ullah J. H., Walsh T. R., Taylor I. A., Emery D. C., Verma C. S., Gamblin S. J. et al. (1998) The crystal structure of the L1 metallo-β-lactamase from *Stenotrophomonas maltophilia* at 1.7 Å resolution. J. Mol. Biol. **284:** 125–136

9 Baldwin G. S., Galdes A., Hill H. A., Smith B. E., Waley S. G. and Abraham E. P. (1978) Histidine residues of zinc ligands in beta-lactamase II. Biochem. J. **175:** 441–447

10 Seny D. de, Heinz U., Wommer S., Kiefer M., Meyer-Klaucke W., Galleni M. et al. (2001) Metal ion binding and coordination geometry for wild type and mutants of metallo-β-lactamase from *Bacillus cereus* 569/H/9 (BcII): a combined thermodynamic, kinetic, and spectroscopic approach. J. Biol. Chem. **276:** 45065–45078

11 Seny D. de, Prosperi-Meys C., Bebrone C., Rossolini G.M., Page M., Noel P. et al. (2002) Mutational analysis of the two zinc-binding sites of the *Bacillus cereus* 569/H/9 metallo-β-lactamase. Biochem. J. **363:** 687–696

12 Prosperi-Meys C., Wouters J., Galleni M. and Lamotte-Brasseur J. (2001) Substrate binding and catalytic mechanism of class B β-lactamases: a molecular modelling study. Cell. Mol. Life Sci. **58:** 2136–2143

13 Pearlman D. C. D., Caldwell J. A., Ross W. S., Cheathman T. E., Ferguson D. M., Seibel G. L. et al. (1986) AMBER 4.1. University of California, San Francisco

14 Galleni M., Lamotte-Brasseur J., Rossolini G. M., Spencer J., Dideberg O. and Frere J. M. (2001) Standard numbering scheme for class B beta-lactamases. Antimicrob. Agents Chemother. **45:** 660–663

15 Li Z., Rasmussen B. A. and Herzberg O. (1999) Structural consequences of the active site substitution Cys181 Ser in metallo-β-lactamase from *Bacteroides fragilis*. Protein Sci. **8:** 249–252

16 Shih H. H. L., Brady J. and Karplus M. (1985) Structure of proteins with single-site mutations: a minimum perturbation approach. Proc. Natl. Acad. Sci. USA **82:** 1697–1700

17 Dewar M. J. S., Zoebisch E. G., Healy E. F. and Stewart J. J. P. (1985) Development and use of quantum mechanical molecular models. 76. AM1: a new general purpose quantum mechanical molecular model. J. Am. Chem. Soc. **107:** 3902–3909

18 Schrauber H., Eisenhaber F. and Argos P. (1993) Rotamers: to be or not to be? An analysis of amino acid side-chain conformations in globular proteins. J. Mol. Biol. **230:** 592–612

19 Chantalat L., Duee E., Galleni M., Frere J.-M. and Dideberg O. (2000) Structural effects of the active site mutation cysteine to serine in *Bacillus cereus* zinc-β-lactamase. Protein Sci. **9:** 1402–1406

20 Yang Y., Keeney D., Tang X.-J., Canfield N. and Rasmussen B. A. (1999) Kinetic properties and metal content of the metallo-β-lactamase CcrA harboring selective amino acid substitutions. J. Biol. Chem. **274:** 15706–15711

21 Zervosen A., Valladares M. H., Devreese B., Prosperi-Meys C., Adolph H.-W., Mercuri P. S. et al. (2001) Inactivation of *Aeromonas hydrophila* metallo-β-lactamase by cephamycins and moxalactam. Eur. J. Biochem. **268:** 3840–3850

22 Nagano R., Adachi Y., Imamura H., Yamada K., Hashizume T. and Morishima H. (1999) Carbapenem derivatives as potential inhibitors of various beta-lactamases, including class B metallo-beta-lactamases. Antimicrob. Agents Chemother. **43:** 2497–2503

23 Walter M. W., Felici A., Galleni M., Soto R. P., Adlington R. M., Baldwin J. E. et al. (1996) Trifluoromethyl alcohol and ketone inhibitors of metallo-β-lactamases. Bioorg. Med. Chem. Lett. **6:** 2455–2458

24 Walter M. W., Valladares M. H., Adlington R. M., Amicosante G., Baldwin J. E., Frere J.-M. et al. (1999) Hydroxamate inhibitors of *Aeromonas hydrophila* AE036 metallo-β-lactamase. Bioorg. Chem. **27:** 35–40

25 Toney J. H., Fitzgerald P. M., Grover-Sharma N., Olson S. H., May W. J., Sundelof J. G. et al. (1998) Antibiotic sensitization using biphenyl tetrazoles as potent inhibitors of *Bacteroides fragilis* metallo-beta-lactamase. Chem. Biol. **5:** 185–196